

Microwave whispering gallery resonator for efficient optical up-conversion

D. V. Strekalov, H. G. L. Schwefel*, A. A. Savchenkov, A. B. Matsko, L. J. Wang*, and N. Yu

*Jet Propulsion Laboratory, California Institute of Technology,
4800 Oak Grove Drive, Pasadena, California 91109-8099*

**Max-Planck-Institute for the Science of Light, D-91058 Erlangen, Germany*

(Dated: May 30, 2019)

Conversion of microwave radiation into the optical range has been predicted to reach unity quantum efficiency in whispering gallery resonators made from an optically nonlinear crystal and supporting microwave and optical modes simultaneously. In this work we theoretically explore and experimentally demonstrate a resonator geometry that can provide the required phase matching for such a conversion at any desired frequency in the sub-THz range. We show that such a ring-shaped resonator not only allows for the phase matching, but also maximizes the overlap of the interacting fields. As a result, unity-efficient conversion is expected in a resonator with feasible parameters.

PACS numbers: 41.20.Jb, 42.65.Wi, 42.65.Ky

Nonlinear frequency conversion of far-infrared or microwave signals into the optical domain has been actively used for detection of such signals [1, 2, 3, 4, 5, 6, 7, 8, 9]. The relative ease of optical signal detection compared to e.g. those in the THz or sub-THz range, in combination with an intrinsically noiseless character of nonlinear frequency conversion, explains the close attention this method has been receiving. Its main drawback, however, is its low conversion efficiency. The highest power conversion efficiency known to us is about 0.5%, which has been only recently achieved [9] for 100 GHz signal using 16 mW of CW optical pump at 1560 nm. This number corresponds to the photon-number conversion efficiency of approximately $2.6 \cdot 10^{-6}$, following the Manley-Rowe relation.

Highly efficient and noiseless upconversion of microwave radiation into the optical domain would open up numerous possibilities in microwave imaging and communications. One example of such a possibility, that we have discussed earlier [9], is microwave photon counting at room temperature. Reaching the photon-counting regime in the sub-THz or THz range would be an achievement important for quantum information processing and computing, sub-millimeter spectroscopy and astronomy, security, and for other areas where the ultimate sensitivity detection of microwave radiation is desired. Unfortunately, even the most efficient up-converter to-date is still seven orders of magnitude short of the photon-counting regime for 100 GHz photons at room temperature [9]. On the other hand, the theoretical analysis [10] shows that this regime can be achieved. The key to its realization is reaching unity conversion efficiency. An all-resonant whispering gallery mode (WGM) configuration of the frequency converter should achieve this goal.

WGM resonators with optical nonlinearity have been successfully used in nonlinear optics in general and in microwave photonics in particular [11, 12, 13, 14]. In a recent experiment [9] a lithium niobate WGM resonator with the optical free spectral range (FSR) $\Omega = 2\pi \cdot 12.64$ GHz was irradiated by a microwave signal with the frequency near $\omega_M = 8 \cdot \Omega \approx 2\pi \cdot 101.12$ GHz. This device

is analogous to a lower-frequency electro-optical modulator [11, 13], except that the microwave signal excites the sidebands not in the pair of adjacent to the carrier optical WGMs, but in those across eight of optical FSRs. To describe the operation of such a modulator, we follow the steps of [13] and introduce the interaction Hamiltonian

$$\hat{H}_i = \hbar g (\hat{b}_-^\dagger \hat{c}^\dagger \hat{a} + \hat{b}_+ \hat{c}^\dagger \hat{a}^\dagger) + c.c., \quad (1)$$

which couples the optical pump and microwave signal WGMs (photon annihilation operators \hat{a} and \hat{c} , respectively) with the Stokes and anti-Stokes optical upconverted signal (\hat{b}_- and \hat{b}_+ , respectively). The coupling constant

$$g = \frac{4\pi\omega}{\varepsilon} \chi^{(2)} \sqrt{\frac{2\pi\hbar\omega_M}{\varepsilon_M V_M}} \left(\frac{1}{V} \int_V dV \Psi_a^* \Psi_b \Psi_c \right) \quad (2)$$

includes the (bracketed) factor describing the overlap between the fields inside the resonator. In Eq. (2), ω , ε and V are optical frequency, dielectric constant and mode volume, respectively; those with the subscript M are similar microwave parameters.

Irradiating the resonator with the microwaves by placing the former near a waveguide opening is a very inefficient method of coupling the microwaves with the optical WGMs, as the main part of the microwave energy reflects back into the waveguide or scatters into space. This problem can be solved by using an all-resonant frequency up-converter, supporting microwave WGMs as well as optical ones. Experimental studies of microwave WGMs in crystalline disks and rings carried out in the 1980's shown remarkable quality factors of $Q \approx 10^{10}$ [15].

For the all-resonant up-converter, all wave functions Ψ in (2) are optical or microwave eigenfunctions of the WGM resonator. Approximating the resonator rim as a piece of a sphere with radius R , we can express them as

$$\Psi = \Psi^{(L,q)}(r, \varphi) = \frac{N}{r} J_{L+1/2}(k_{L,q} r) e^{iL\varphi}, \quad (3)$$

where N is a normalization factor, L and q are orbital and radial numbers, and the wavenumbers $k_{L,q} = n\omega/c$ are solutions to the WGM dispersion equation [13].

The Hamiltonian (1) and equations (2) and (3) lead to the following phase-matching conditions:

$$\omega_M = L_M \Omega \quad \text{and} \quad L_M = |L_s - L_p|, \quad (4)$$

where L_M , L_s and L_p are the orbital momenta of the microwave, optical signal (Stokes or anti-Stokes), and pump WGMs, respectively. Below we show that conditions (4) can be satisfied for any desired microwave frequency by taking advantage of the strong waveguide dispersion of the microwave mode.

Once the phase-matching conditions are fulfilled, the microwaves-to-optics conversion will be efficient as long as the nonlinear coupling rate exceeds the loss rate in the microwave WGM, that is, if the total loss rate of the THz mode $\gamma = \gamma_{nl} + \gamma_{abs}$ is dominated by the rate of nonlinear frequency conversion γ_{nl} . Experimentally this means that the microwave WGM resonances will be considerably broadened when the optical pump is turned on. Then if the optical WGMs couple strongly to the input and output free-space beams (i.e. the resonator is optically over-coupled) the unity-efficient conversion is theoretically possible [10].

To estimate the conversion efficiency, we use the result by [13] for the ratio of the optical sidebands powers P_{\pm} to the pump power P_0 :

$$\frac{P_{\pm}}{P_0} = \left(\frac{2\xi\sqrt{P_M}}{1 + 2\xi^2 P_M} \right)^2, \quad \xi = \frac{4gQ}{\omega} \sqrt{\frac{Q_M}{\hbar\omega_M^2}}, \quad (5)$$

where Q and Q_M are the optical and microwave WGM quality factors, respectively, and P_M is the microwave power. We are interested in very low microwave powers, eventually at the single photon levels, which allows us to make the approximation $1 + 2\xi^2 P_M \approx 1$. Then we turn Eq. (5) around and find the up-conversion efficiency:

$$\frac{\langle N_{\pm} \rangle}{\langle N_M \rangle} = \frac{P_{\pm}}{P_M} \frac{\omega_M}{\omega} \approx 4\xi^2 P_0 \frac{\omega_M}{\omega}. \quad (6)$$

Below we show that for an optimally chosen geometry of the WGM resonator, the photon-number conversion efficiency (6) may approach unity at as low optical pump power as $P_0 = 6$ mW. Near the unity conversion efficiency the estimate (6) may not be accurate, and saturation effects need to be taken into account. However the purpose of our estimate is to show that nearly absolute conversion efficiency can be achieved even with modest assumptions concerning the system parameters.

Previously [16] we have observed lower frequency microwave WGMs in lithium niobate disks in the 30 GHz range. The relatively long wavelength of these microwaves allowed for direct observation of WGM field distribution using an absorbing probe. One important conclusion of this study has been that the microwave WGMs have poor spatial overlap with the optical modes that occupy just few tens of microns near the disk rim. This may greatly reduce the overlap factor in (2). Although this problem is less severe for higher frequencies and higher

orbital numbers, it still may severely impede achieving high conversion efficiency. Therefore we have proposed using ring resonators instead of the disks. When filled with a low-constant dielectric, such rings tend to concentrate the microwave field inside themselves, forcing a good overlap with the optical WGMs.

In the following we assume that the optical axis of lithium niobate is perpendicular to the disk plane, and that the microwave as well as optical fields are polarized along the optical axis. Then the largest nonlinearity coefficient of lithium niobate d_{33} is utilized for microwave-to-optics conversion.

Efficient coupling of the optical WGMs to the optical pump requires the external rim of the ring to be shaped as a spheroid with the radii ratio equal to [9]

$$\rho/R = (n_p^2 - n^2)/n_p^2, \quad (7)$$

where n_p is the refraction index of the prism used for the optical coupling. If the prism is made of diamond and the pump has the wavelength $\lambda = 1550$ nm, then $n_p = 2.384$ while $n = 2.138$, which yields $\rho/R = 0.196$.

To demonstrate how the phase-matching conditions (4) can be satisfied in this geometry, we find the optical FSR $\Omega \approx c/(nR)$ and plot the phase-matching curve $\omega_M(L_M)$ as follows from the first equation of (4), together with the microwave dispersion curve, in Fig. 1. Intersection of the two curves at an integer value of L_M indicates that phase-matching is achieved. The accuracy to which the two frequencies should match at this value of L_M is determined by the smaller of the optical and microwave WGM linewidths. Notice that the microwave dispersion curve (B) in Fig. 1 depends on all four geometric parameters of the ring, while the phase-matching curve (A) depends only on the external radius R . This gives us enough freedom to achieve the phase-matching at a desired microwave frequency. In the example shown in Fig. 1 the phase-matching was found for $\omega_M = 2\pi \cdot 100.0$ GHz at

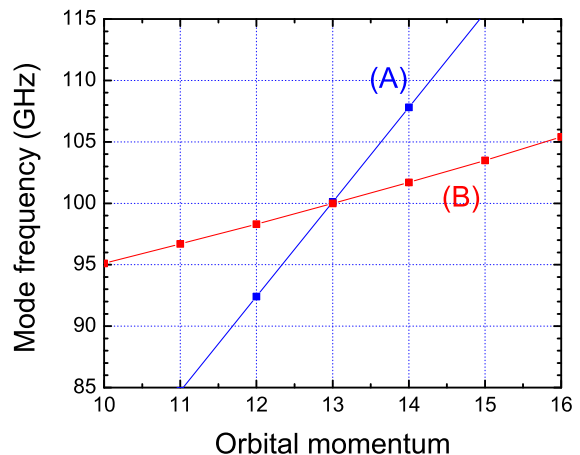


FIG. 1: A phase-matching solution for $\omega_M = 2\pi \cdot 100$ GHz found at $L_M = 13$. Curve (A) is the phase-matching curve resulting from Eq. (4); curve (B) is the microwave dispersion curve calculated numerically.

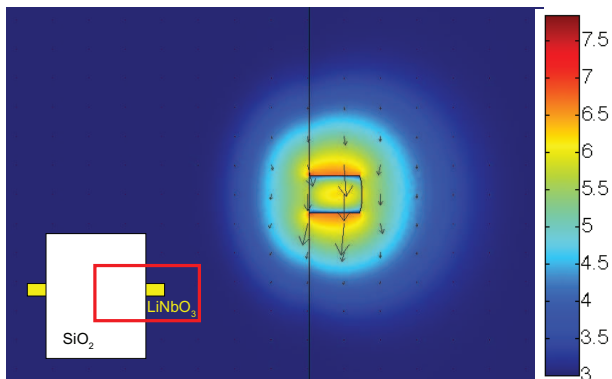


FIG. 2: Absolute value of the E_z -component of a microwave WGM mode with $\omega_M = 2\pi \cdot 100$ GHz, $L_M = 13$. The plot is on a log scale with color map given on the right. A sketch of the geometry is shown in the inset, where the red box represents the calculation window.

$L_M = 13$. The ring thickness was $h = 292 \mu\text{m}$, its inner and outer radii were $R_{in} = 2.48$ mm and $R = 2.9$ mm, respectively. $R = 2.9$ mm yields $\rho = 568 \mu\text{m}$.

The microwave dispersion curve is obtained by numerical simulation. These simulations have been carried out in a finite element solver, COMSOL [17] adapting an axis symmetrical formulation by Oxborrow [18]. Fused silica was selected as the post material because of its low microwave absorption and relatively small dielectric constant at 100 GHz $n=1.9$, compared to the much higher dielectric constant of lithium niobate $n_e=5.15$ and $n_o=6.72$. In this configuration the microwave field is strongly concentrated inside of the lithium niobate ring (see Fig. 2), which provides both good coupling with the external waveguide and good overlap with the optical field.

Our numerical simulations also allow us to determine the coupling constant (2) and the conversion efficiency (6). To carry out this estimate we notice that the eigenfunctions of the optical modes in (2) are practically equivalent, $\Psi_a \approx \Psi_b$, and that the microwave eigenfunction Ψ_c can be treated as a constant and taken out from the integral. This constant is found from the numerical simulation. We further notice that the “mode volume” is defined as a volume integral of the absolute square of the eigenfunction. Therefore the optical mode volume drops out, while the microwave mode volume is found by numerical integration of the simulation data. To complete the estimate we take the optical frequency $\omega = 1.2 \cdot 10^{15} \text{ s}^{-1}$ ($\lambda = 1.55 \mu\text{m}$), the dielectric susceptibilities $\varepsilon = 4.6$ and $\varepsilon_M = 26$, $\chi^{(2)} = 10^{-6}$ (cgse units) [13], $Q = 10^8$ and $Q_M = 100$. Substituting these numbers into Eq. (6) we find the photon-number conversion efficiency approaching unity already at a 6 mW optical pump.

To demonstrate the WGM ring resonators in an experiment, we machined a ring closely matching the parameters calculated above and mounted it on a slightly tapered fused silica post as shown in Fig. 3. In this experiment the outer rim of the ring was shaped as a cylinder ($\rho = \infty$) instead of a spheroid, which had little effect on

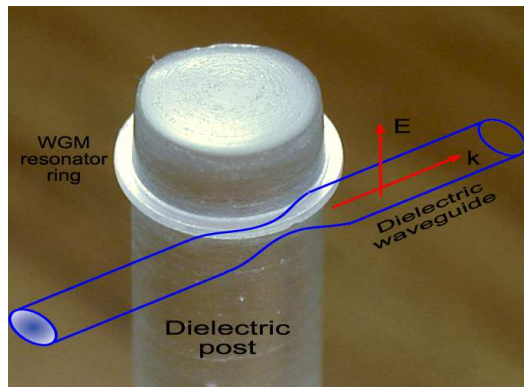


FIG. 3: A lithium niobate WGM ring resonator mounted on a fused silica post (photo) coupled with a tapered dielectric waveguide (drawing). The ring height is 0.29 mm, outer radius is 2.9 mm.

its microwave spectrum. At the mounting location, the outer radius of the silica stem was 2.48 mm. However due to the roughness and tapering caused by the drilling process, the effective inner radius of the lithium niobate ring was slightly larger. In our analysis we treated this radius as a free parameter and found an excellent agreement between the numerical simulations and experimental data for $R_{in} = 2.61$ mm.

The outer radius of the lithium niobate ring initially measured 2.99 mm. Microwaves were supplied by a tapered dielectric waveguide coupling to the resonator through the evanescent field. This technique allowed us to achieve the optimal coupling with the resonator WGMs by translating the resonator along the waveguide. In this experiment we used a fused silica rod stretched over a hydrogen torch to approximately half of its initial diameter of 3 mm.

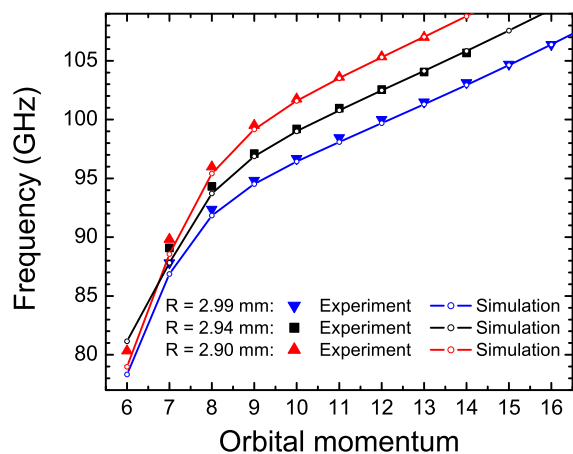


FIG. 4: Dependence of the microwave spectrum on the resonators outer radius. The experimental data and theoretical calculations done by finite element method show very good agreement for the effective inner radius determined to be $R_{in} = 2.61$ mm.

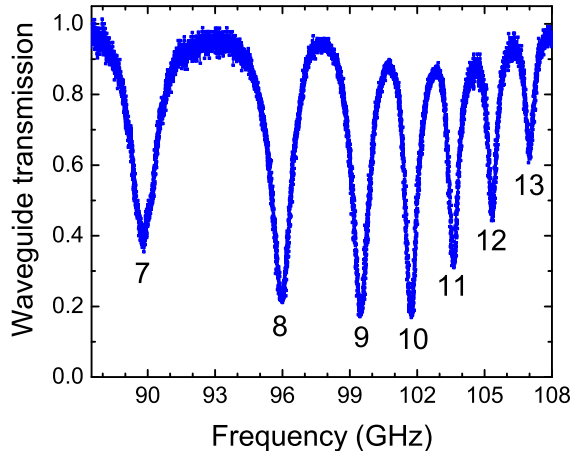


FIG. 5: Microwave spectrum of the ring resonator shown in Fig. 3. The modes are labeled by the orbital number L_M .

We gradually polished the disk rim, reducing the outer radius from 2.99 to 2.90 mm. The resulting dispersion curves were therefore shifted, see Fig. 4. The thin ring in our experiment acts as a looped single-mode microwave waveguide. Therefore the mode sequence in Fig. 4 is indexed by the orbital number L_M determined from the numeric simulation. The simulated dispersion curves are also shown in Fig. 4.

The microwave spectrum for the final value $R = 2.90$ mm is shown in Fig. 5. From this spectrum we see that signal coupling from the THz waveguide into the res-

onator as high as 82% was achieved. We determine the microwave WGM quality factor to be $Q \approx 100$.

It is important to point out that the purpose of the numeric simulation is not to achieve the exact phase-matching, but only to unambiguously determine the angular momentum L_M . An error small compared to the microwave FSR would be tolerable, because the phase matching can be fine-tuned via modifying the microwave dispersion of the system. For example, placing a metal ring on the fused silica post near the resonator ring, we have been able to tune the microwave frequency by more than 0.5 GHz without appreciable degradation of the quality factor.

To summarize, we have studied microwave WGMs in the ring resonators. The purpose of this study has been to determine the utility of such systems as efficient microwave-to-optics converters, with the focus made on efficient coupling of microwaves into the resonator's WGMs; improving the overlap between the microwave and optical fields; and theoretical demonstration of the phase-matching for desired signal frequency. All of this has been achieved, and we believe that the actual demonstration of nearly unity-efficient microwave-to-optics conversion with subsequent optical photon counting is now feasible. The benefits from its practical implementation are expected in the areas of quantum information (e.g., quantum computing with quantum electronic circuits), astronomy and spectroscopy.

The experimental research described in this paper was carried out at the Jet Propulsion Laboratory, California Institute of Technology, under a contract with the NASA.

-
- [1] W. C. Chiou and F. P. Pace, *Appl. Phys. Lett.* **20**, 44 (1972).
 - [2] M. M. Abbas, T. Kostiuk, and K. W. Ogilvie, *Appl. Opt.* **15**, 961 (1976).
 - [3] M. A. Albota and F. N. C. Wong, *Opt. Lett.* **29**, 1449 (2004).
 - [4] K. Karstad, A. Stefanov, M. Wegmuller, H. Zbinden, N. Gisin, T. Aellen, M. Beck, and J. Faist, *Opt. Lasers Engineer.* **43**, 537-544 (2005).
 - [5] G. Temporao, S. Tanzilli, H. Zbinden, N. Gisin, T. Aellen, M. Giovannini, and J. Faist, *Opt. Lett.* **31**, 1094-1096 (2006).
 - [6] A. P. VanDevender and P. G. Kwiat, *J. Opt. Soc. Am. B* **24**, 295-299 (2007).
 - [7] Y.J. Ding and Wei Shi, *Solid-State Electron.* **50**, 1128 (2006).
 - [8] M.J. Khan, J.C. Chen and S. Kaushik, *Opt. Lett.* **32**, 3248-50 (2007).
 - [9] D. V. Strekalov, A. A. Savchenkov, A. B. Matsko and N. Yu, *Opt. Lett.* **34**, 713-715 (2009).
 - [10] A. B. Matsko, D. V. Strekalov and N. Yu, *Phys. Rev. A*, **77**, 043812 (2008).
 - [11] D. A. Cohen and A. F. J. Levi, *Electron. Lett.* **37**, 37-39 (2001).
 - [12] P. Rabiei, W. H. Steier, C. Zhang, and L. R. Dalton, *L. Lightwave Technol.* **20**, 1968-1975 (2002).
 - [13] V. S. Ilchenko, A. A. Savchenkov, A. B. Matsko, and L. Maleki, *JOSA B* **20**, 333-342 (2003).
 - [14] M. Hossein-Zadeh, and A. F. J. Levi, *IEEE Trans. Microwave Theor. and Techniques* **54**, 821-831 (2006).
 - [15] V.B. Braginsky, V.S. Ilchenko, and Kh.S. Bagdassarov, *Phys. Lett. A*, **120**, 300-305 (1987).
 - [16] D. V. Strekalov, A. A. Savchenkov, A. B. Matsko and N. Yu, *Laser Phys. Lett.*, **6**, 129 (2009).
 - [17] COMSOL Multiphysics User's Guide Version 3.5, COMSOL AB, Stockholm, Sweden, 2008.
 - [18] M. Oxborrow, *IEEE T. Microw. Theory* **55**, 1209-1218 (2007).